

Microstructural studies of Ag and Ag alloy sheathed Tl-1223 tapes

Pavel Diko,^{*a} Simon Fox,^b Jo C. Moore,^b Chris R. M. Grovenor^{*b} and Mike J. Goringe^b

^aInstitute of Experimental Physics, SAS, Watsonova 47, Kosice, Slovakia

^bDepartment of Materials, Oxford University, Parks Road, Oxford, UK OX1 3PH

The influence of processing conditions on the grain size, alignment and connectivity, porosity, secondary phase content and presence of extended defects in PIT Tl-1223 tapes has been studied for samples prepared by both sintering and *in situ* reaction mechanisms. Tape thickness reduction by cold rolling resulted in grain refinement due to precursor or 1223 particle crushing, and some grain alignment especially in tapes prepared by *in situ* reaction. By contrast, an increase in grain connectivity was observed in rolled tapes prepared by sintering. The abnormal grain growth of 1223 crushed grains was observed in the case of tapes prepared by sintering. An increase in secondary phase content observed during extended annealing is related to thallium loss. Shear defects were formed at higher rolling deformations, and suggested to be particularly detrimental for transport currents.

The low irreversibility fields of Bi-based 2212 and 2223 superconductors limit their applications, at least at temperatures above *ca.* 30 K. Thallium-based high-temperature superconductors of the 1223 composition, typically $Tl_x(Bi/Pb)_y(Sr_{0.8}Ba_{0.22})_2Ca_2Cu_3O_\delta$, is a candidate material for operation at significant magnetic fields at 77 K because of their high irreversibility fields.¹⁻³ The most commonly used technique for the fabrication of Tl-1223 superconducting wires in long lengths is the powder in tube (PIT) method. Superconducting critical current densities (J_c) of the order of 10^4 A cm⁻² have been achieved in self field at 77 K in (Tl,Pb)-1223^{4,5} and (Tl,Bi)-1223^{6,7} PIT tapes. However, as yet, weak links (which may lie between the superconducting Tl-1223 grains) represent a serious problem for large-scale application.^{8,9} In applied magnetic fields J_c values may drop to a few percent of their zero field value due to weak links in the polycrystalline tapes.^{4,6,8,10} Self field effects have also been shown to be very important in controlling the current carrying properties of these tapes.¹¹ Weak links have to be strengthened by improving either crystallite alignment or grain connectivity.

The processing routes most extensively used to fabricate Tl-1223 PIT tapes can be divided into two types; sintering and an *in situ* reaction process. The first process uses fully reacted Tl-1223 superconducting powder where the individual grains are sintered together in the final annealing step. The *in situ* reaction process uses a precursor containing BaCuO₂, (Sr/Ca)Cu oxides and CuO mixed with Tl and Pb (or Bi) oxides which reacts to form the 1223 phase inside Ag tape. Most groups report higher J_c values and improved field dependences for *in situ* reaction routes.^{4,6,8} However, surprisingly little information on microstructural development during deformation and annealing steps is available in the literature, although impurity phase analysis by transmission electron microscopy and some work on the microstructural effects of rolling and pressing has been reported by Miller *et al.*¹² We report here on a study primarily by optical microscopy on the influence of starting powder and thermal-mechanical processing methods on the microstructure and transport properties of Tl-1223 tapes. Particular emphasis will be placed on the analysis of the degree of grain alignment and volume fractions of porosity and impurity, or secondary, phases.

Experimental

Tape samples were fabricated using either fully reacted superconducting powder or a partly reacted precursor mixture, and the overall composition was $(Tl_{0.78}Bi_{0.22})(Sr_{0.8}Ba_{0.22})_2$

$Ca_2Cu_3O_\delta$ in both cases. For all the powders, a precursor was fabricated from SrCO₃, BaO₂, CaO and CuO by heating at 940 °C for 16 h, regrinding and repeating the procedure three times. Tl₂O₃ and Bi₂O₃ were then added in stoichiometric amounts to form the precursor mixture.¹¹ Superconducting powder was made by reacting this mixture in a sealed alumina crucible at 940 °C for 2 h. This powder is approximately 95% pure as estimated by X-ray diffraction and has an average grain size of 10 μm.¹³ Tape samples were fabricated using the usual powder in tube technique. The powders were packed into silver or AgNiMg alloy tubes and then drawn to a diameter 1.5 mm and cold rolled to their final thickness. The last annealing step was in air under the conditions specified below.

Longitudinal (L), transverse (TR) and tilted (TT) sections of the tapes were prepared for microscopical analysis by conventional metallurgical polishing. Tilted sections (about 5° declination from the tape surface) provide information similar to sections parallel to the tape surface. After fine polishing, the microstructure of the samples was investigated by optical microscopy in normal and polarised light. A Laves-Ernst (LE) compensator was also used to optimise the visualisation of interesting microstructural details. The volume fractions of both porosity and of secondary phases were estimated by a point counting method.¹⁴ Changes in Tl-1223 grain alignment were studied by estimating from optical micrographs the volume fraction of the characteristically shaped 1223 platelet grains lying with their *c*-axes perpendicular to the tape length. The polarizers, LE compensator and sample on the stage were set into positions in which the 1223 platelets with this alignment in the tape appear blue. The angular selectivity of this method is not better than 10°, but allows an approximate measure of the degree of *c*-axis alignment in different parts of the same tape. Scanning electron microscopy with energy dispersive X-ray microanalysis (EDX) was also used for the study of the approximate composition of the impurity phases. The critical current (I_c) values for all the tapes were determined by the usual four-point measurement technique using a voltage criterion of 1 μV cm⁻¹.

Results and Discussion

We have chosen to study the influence of specific processing variables such as final tape thickness, rolling reductions per pass and final annealing time on the microstructure of the Tl-1223 tapes. Results on each variable will be presented separately.

Influence of final tape thickness

The first set of samples was prepared by filling AgNiMg alloy tubes with the unreacted precursor powder described above. The tubes were mechanically processed to tape 150 μm thick by drawing and rolling, and were then annealed for 30 min at 840 $^{\circ}\text{C}$. Tapes of final thicknesses in the range 150–75 μm were then prepared by rolling and given a last *in situ* reaction process at 840 $^{\circ}\text{C}$ for 7.5 h in air (tape A).

The microstructure of the superconducting core in these tapes consists principally of platelets of the Tl-1223 superconducting phase, larger (Ca,Sr)Cu oxide phases and small rounded Ag particles (Plate 1). These three materials have very characteristic contrasts in the optical microscope, and this allows very rapid assessment of phase purity. EDX microanalysis in the scanning electron microscope indicates that most of the secondary phase particles are of approximate stoichiometry (Ca,Sr)CuO₂ or (Ca,Sr)₂CuO₃. These are the same majority secondary phases as identified by Miller *et al.* in rather similar tapes.¹² We also observe particles of a Tl+Ag+Ca-rich phase in many of our tapes,¹⁵ presumably the same one as identified by Mogro-Campero *et al.*¹⁶ in 1223 thick film samples.

The (Ca,Sr)Cu oxide secondary phase particles are frequently developed at the interface between the superconducting core and AgNiMg sheath, forming sometimes a compact interlayer, Plate 2(a) and (b). This interlayer was thicker and more developed in the thinnest tapes. The formation of this layer of

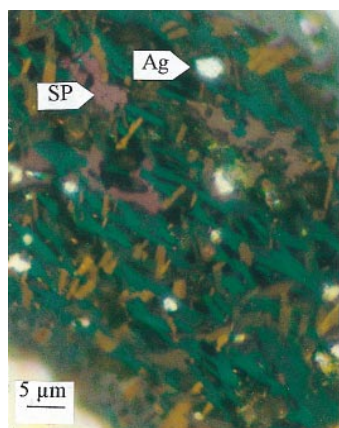


Plate 1 Longitudinal section of tape A (110 μm thick) imaged with polarised light showing a typical distribution of 1223 platelets, secondary phase (SP) and silver particles

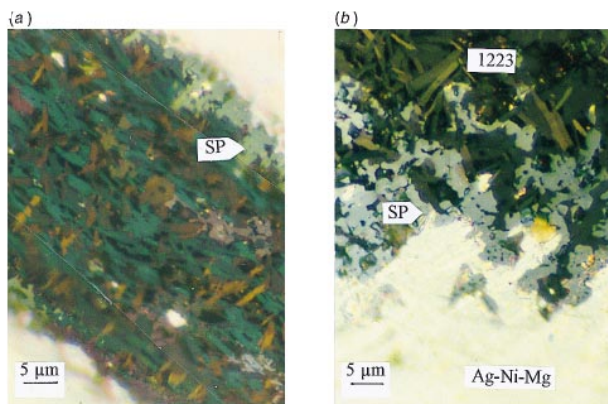


Plate 2 (a) Longitudinal section of tape A (75 μm thick) imaged with polarised light. Blue 1223 platelets have their *c*-axis approximately perpendicular to the tape length. A rather continuous SP layer can be seen at the superconductor/AgNiMg alloy interface. (b) Tilted section of tape A (150 μm thick) imaged with normal light. The SP can again be seen to be concentrated at the superconductor/AgNiMg alloy interface

secondary phase may be associated with thallium loss through the open ends of short annealed tape samples, since similar concentrations of secondary phases are formed at the ends of the tapes as well. However, the loss of Tl by diffusion through the sheathing Ag alloy, its oxidation at the outer surface and evaporation from the sheath surface cannot be excluded. The significant solubility of Tl in Ag (4 atom% at 840 $^{\circ}\text{C}$ according to Barron¹⁷) and high diffusion rate of Tl in Ag at 840 $^{\circ}\text{C}$ ¹⁸ ($D_{840} = 5 \times 10^{-9} \text{ cm}^2 \text{ s}^{-1}$) support the idea of Tl loss through the sheath. Tl depletion during annealing can perhaps explain the shift of the maximum critical current values to lower tape thickness in the case of the tapes containing 20% Tl₂O₃ excess, Fig. 1. The thinner tapes have reduced levels of porosity (see below) which increases the average I_c values, but Tl loss from a smaller volume of core in the thinner samples can have a serious counter effect on the I_c values unless the excess Tl is added. (It is also possible that the addition of the excess Tl alters the mechanical properties of the core thereby limiting the formation of deformation cracks of the type described below.)

The mean size of the Tl-1223 platelets, characterised by length measurements on the optical sections, decreases with the tape thickness, Fig. 2. The platelet refinement may be

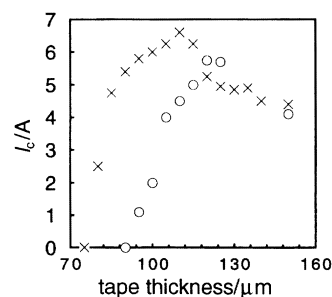


Fig. 1 I_c values plotted *vs.* thickness for tapes of type A of nominal stoichiometric composition (\circ) and with 20% Tl₂O₃ excess (\times). The tapes with the excess of Tl perform much better than the stoichiometric ones at thicknesses below about 100 μm .

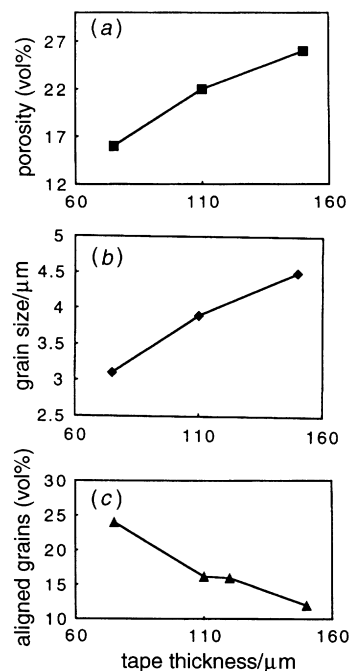


Fig. 2 Core porosity, 1223 platelet length and volume fraction of aligned 1223 platelets plotted *vs.* final tape thickness for tapes of type A. The errors on all these measurements are estimated to be at least $\pm 0.5 \mu\text{m}$ in length, $\pm 5\%$ in porosity and $\pm 5\%$ in the volume of aligned grains, but the general trends are clear.

caused by reduction of the precursor grain size by mechanical deformation during rolling. As the tape thickness is reduced, the Tl-1223 grain alignment slightly improves, but the bulk of the core is still not well aligned with only about 25% of the grains lying with their *c*-axes within $\pm 10^\circ$ of the vertical axis of the tapes, Fig. 2. Thickness reduction, however, has a more positive influence on the densification of the superconducting core. The porosity is reduced from 26 to 16% as the tape thickness is reduced to 75 μm , Fig. 2.

Two kinds of macrodefects were observed in the superconducting core. Longitudinal macrocracks parallel to the tape surface were occasionally present in samples of all thicknesses, Plate 3(a). Due to their orientation they should have no significant effect on I_c values. More detrimental are shear defects observed in the thinnest tapes, Plate 3(b). They are formed on the planes of maximum shear stress during rolling, and the superconducting path is clearly severely interrupted. These defects are likely to be the main reason why the I_c values fall to zero in the thinner tapes, Fig. 1. Finally, some cracks were observed in the AgNiMg sheath, and the core adjacent to such cracks is seriously depleted in Tl and is converted nearly completely into impurity phases, Plate 3(c).

Influence of rolling reduction per pass. Tapes were prepared by filling both pure Ag and AgNiMg alloy tubes with fully reacted Tl-1223 powder (tape B). Different rolling reductions from 2.5 to 80% were used to fabricate tapes with a nominal final thickness of 250 μm . At the higher reductions one or two passes were sufficient to reduce the drawn round wire to this thickness, but obviously at the low reductions a very large number of passes was necessary. Some of the tapes sheathed by AgMgNi alloy were rolled in just one pass with very high rolling reductions (tape C). The thickness of these tapes varied significantly because of the unstable mechanical conditions during this kind of severe processing. All this set of tapes was

given a final sintering at 820°C for 30 min. The aim of the work on this set of samples was to study the influence of the rolling reduction on I_c values, Fig. 3, and to explain the rapid drop of I_c at the highest thickness reductions in the case of samples rolled in one pass by investigating any changes in microstructure.

The optical microscopy observations are summarised in Fig. 4. Decreasing porosity can probably explain the higher critical currents measured in samples fabricated with higher rolling reductions, Fig. 3. The Tl-1223 grain size and extent of grain alignment were only slightly influenced. Defects caused by high inhomogeneous shear deformation were found in samples rolled in one pass with reductions greater than 80%, Plate 4. The width of these defects is greater at the highest rolling reduction (90%+). The decrease in I_c values shown for the samples prepared with high rolling reductions is then caused by these shear defects which cannot be fully repaired by sintering during a final heat treatment.

Influence of annealing time

Significant microstructural changes are expected to occur in tapes containing unreacted precursor powder as the sintering time is increased. In order to investigate these changes, tapes

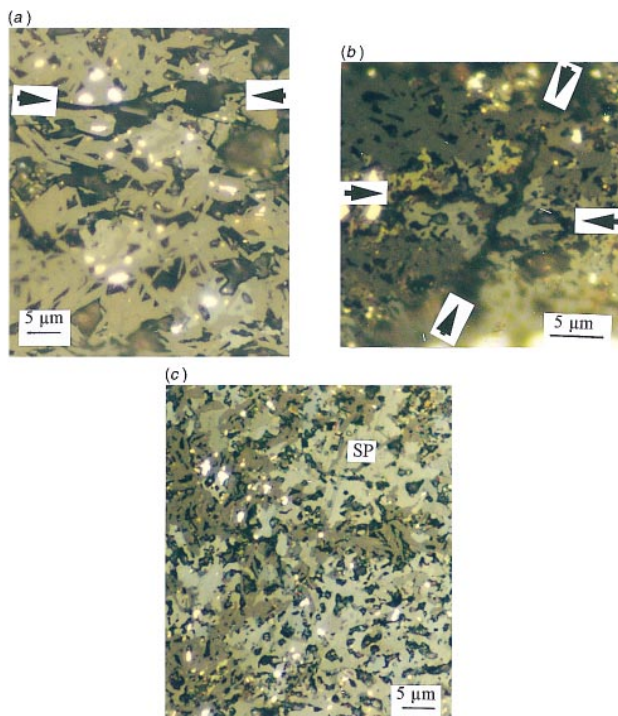


Plate 3 (a) Longitudinal section of tape A (145 μm thick) imaged with normal light showing a macrocrack (arrowed) lying parallel to the tape surface. (b) Longitudinal section of tape A (75 μm thick) imaged with normal light showing both a longitudinal crack running horizontally across the image and a diagonal shear crack. (c) Transverse section of tape A (75 μm thick) imaged with polarised light showing the large volume fraction of SP formed near a crack in the AgNiMg sheath

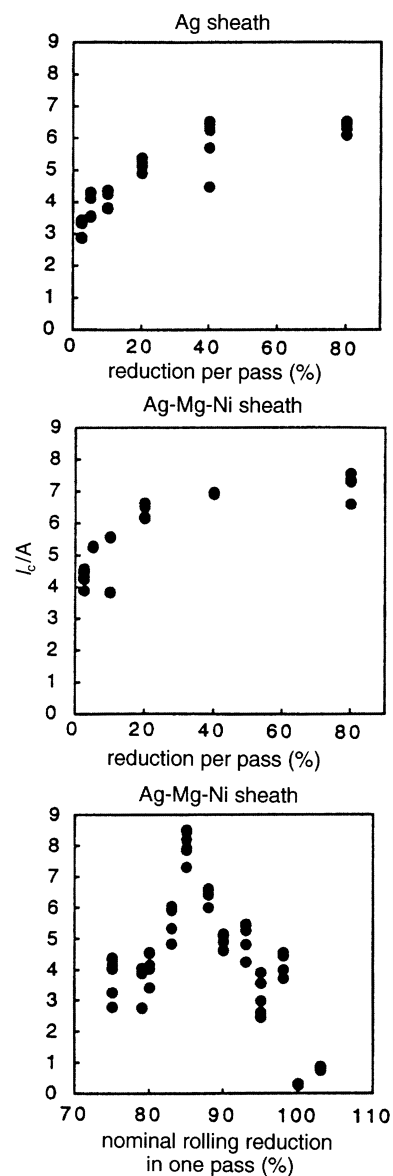


Fig. 3 I_c vs. thickness reduction measurements for tapes containing fully reacted 1223 powder (type B)

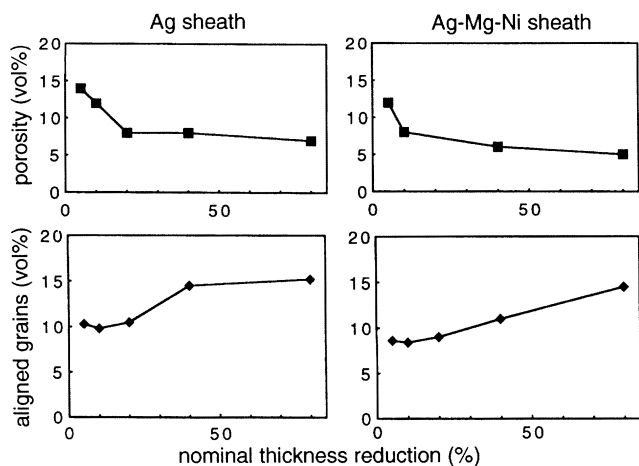


Fig. 4 Core porosity and volume fraction of aligned 1223 platelets plotted vs. rolling reduction for tapes containing fully reacted 1223 powder (type B). In this data only the decrease in porosity with increasing rolling reduction is considered to show a significant variation.

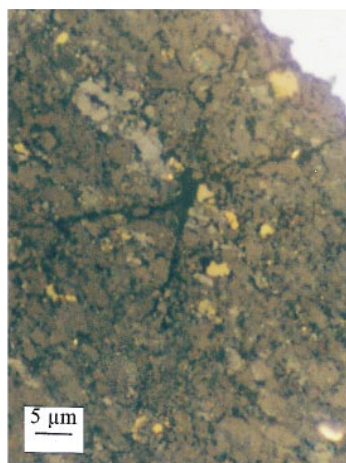


Plate 4 Longitudinal section of sintered 1223 tape (type C) imaged with polarised light showing shear defects in the tapes after nominal 100% rolling reduction in one pass

were prepared in pure Ag tubes by a three-stage reaction and mechanical deformation procedure that has been described in detail elsewhere¹⁹ (tape D). In these previously reported experiments, the critical current values of these tapes have been found to increase with annealing time reaching maximum values after 5–6 h (ref. 17, Fig. 5). The I_c values decrease slightly at higher annealing times.

Under the optical microscope it is clear that annealing leads to densification of the superconducting core by reaction and sintering processes. The porosity in the core decreases from 16% after 6 min final stage annealing to 6% after 10 h, Fig. 5. It is worth noting that Miller *et al.*¹² report very similar levels of porosity in *in situ* reacted Tl-1223 tapes. The densification is accompanied by pronounced 1223 grain growth, Fig. 6 and Plate 5, although the 1223 grains do not have as pronounced a platelike shape as in the case of tapes of type A. This is because the platelets formed in the early annealing stages are crushed during subsequent deformation procedures. The alignment of the Tl-1223 grains is weak in all the samples, and is only slightly improved by longer annealing, Fig. 5.

The mean Tl-1223 grain size is below 0.5 μm in specimens given a short final stage annealing, Fig. 5. It is then not surprising that the grain growth process is abnormal; some grains grow much faster than others. Such grain growth is typical for powder compacts with fine starting grains.²⁰ Abnormal grain growth results in a bimodal (duplex) grain

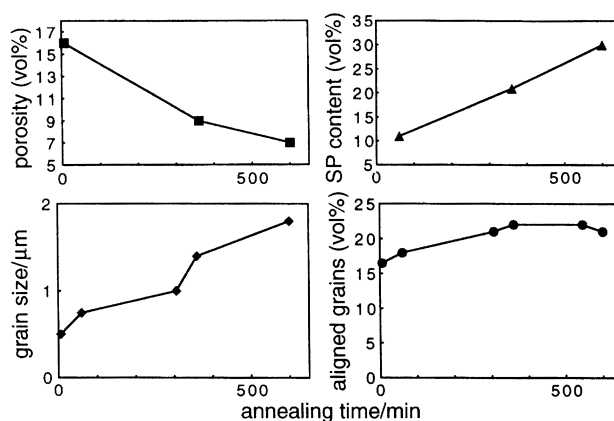


Fig. 5 Core porosity, volume fraction of secondary phase, 1223 platelet length and volume fraction of aligned 1223 platelets plotted vs. annealing time for tapes of type D

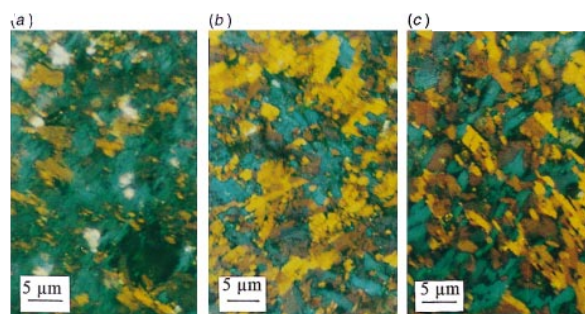


Plate 5 Transverse section of tape D imaged with polarised light after annealing in the final stage at 840°C for (a) 60 min, (b) 306 min and (c) 600 min. A bimodal grain size distribution is found in the 306 min sample which disappears in the later samples.

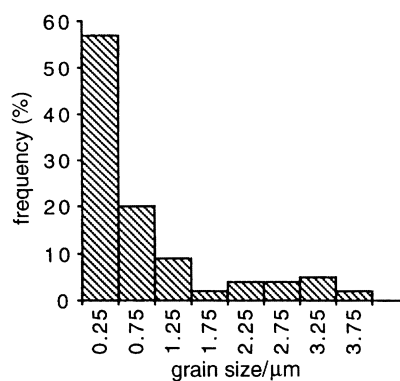


Fig. 6 Frequency distribution chart for grain size in tapes of type D annealed for 306 minutes showing the bimodal distribution with a minor peak at about 3 μm

size distribution (GSD). For tape annealed for 306 min one grain size maximum is at 0.5 μm and the second at *ca.* 3 μm, Fig. 6. The bimodal grain size distribution may offer some promise for reducing the weak link problem in Tl-1223. Magnetic measurements in $YBa_2Cu_3O_{7-x}$ samples have shown that the density of strongly linked grain boundaries is much higher in samples with a bimodal GSD than in polycrystalline ceramic samples with a narrow GSD.^{21,22} It may be significant to note that in our Tl-1223 tapes annealed for the longest times the GSD loses its bimodal character, Plate 5(c).

The dominant secondary phase present in tape D samples was a phase of similar composition to that found in tapes of type A. Surprisingly, no preferential growth of this phase at the Ag/SC interface was observed, and this may be related either to differences in the nucleation efficiency of cuprate

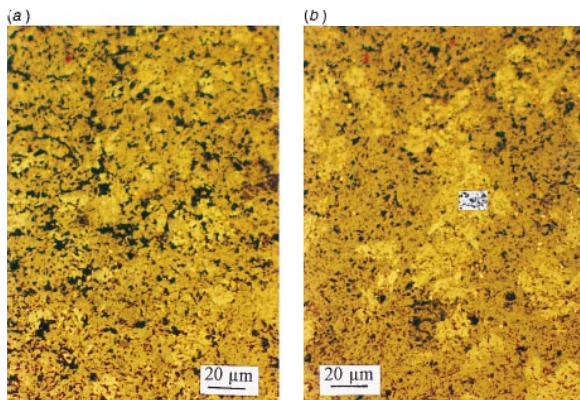


Plate 6 Tilted section of tape D imaged with polarised light after (a) 60 and (b) 600 min final stage annealing. The increase in size and volume fraction of the pale SP is clear. The porosity is also significantly reduced.

impurity phases on pure Ag and AgNiMg alloy surfaces or to different rates of thallium diffusion through the pure silver and the alloyed sheath material. If the rate of diffusion of the thallium is much lower in the pure silver, then the primary mechanism for loss of thallium may no longer be through the sheath and the impurities no longer concentrated at the core/sheath interfaces. However, the volume fraction of this impurity phase increases significantly with the annealing time being 10 vol% after 6 min and as high as 30 vol% after 10 h at 840 °C, Plate 6. The size of the individual colonies of impurity particles can also be seen to increase markedly with annealing time.

If Tl loss through the Ag sheath is significant, some Tl should be detectable in the Ag sheath material adjacent to the core. A measurable Tl content (1–2 atom%) was detected by energy dispersive analysis of tilted sections only in the sheath very close to the Ag/1223 interface. The absence of Cu or Ca peaks in the EDX spectrum taken from the silver sheath close to the core confirms that X-rays generated in 1223 are not contributing significantly to this experiment. Tl was not detected in the silver sheath farther from the Ag/core interface. It could be that the overall kinetics of Tl loss through the Ag sheath are controlled by decomposition of the Tl-1223 phase at the Ag/core interface, and that Tl diffusion through the Ag sheath and Tl_2O_3 evaporation from the surface are much faster processes. There remains a considerable amount of work to be done to understand the dynamics of the Tl mobility during annealing in any detail.

In the light of this microstructural analysis, it is possible to relate the measured critical current variations during annealing primarily to chemical reactions and sintering improving contacts between superconducting grains. The increase in the volume fraction of secondary phases at longer annealing times has an opposing effect on I_c values by reducing the cross-sectional area of superconductor in the tapes. The observed relationship between I_c and annealing time is the result of the balance between these two processes.

Melt processed Tl-1223 tapes

One possible way to reduce the number of weak links in a Tl-1223 tape is by increasing the grain size substantially, and even more importantly by inducing more grain alignment. We have been investigating the melt processing of Tl-1223, and the precise heating sequences used reliably to prepare large grained Tl-1223 tapes have been presented elsewhere.¹⁵ Plate 7 shows a typical polarised light optical micrograph of the microstructure of a partially melted tape. The 1223 grains are blue or brown in this image, while the secondary phases are pink or pale green, and it is clear that both phases are very substantially larger than in any of the previous micrographs.

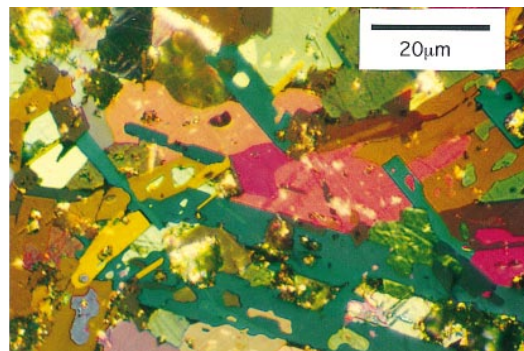


Plate 7 Longitudinal section of partially melted tape imaged with polarised light showing the increase in Tl-1223 and SP grain size

There is, unfortunately, little indication of significant 1223 grain alignment. The critical current values in melted tapes of this kind are very similar to those measured in *in situ* reacted tapes, and so any advantage from the larger 1223 grain size is negated by the larger SP particles blocking the superconducting current path.

Conclusions

Polarised light optical microscopy has been shown to be very effective in visualising superconducting grains and secondary phases in Tl-1223 tapes, allowing the characterisation of grain size, morphology and alignment as well as the observation of defects in the superconducting core. Several observations of relevance to the critical current carrying potential of the tapes have been made.

(1) The alignment of the Tl-1223 grains is rather poor in all the samples investigated in this work although several quite different thermal-mechanical routes have been used to fabricate them. The greatest improvement is achieved by rolling *in situ* reacted tapes to thicknesses below 100 μm. The lack of grain alignment remains the major obstacle to practical application of Tl-based PIT conductors.

(2) The measured critical current values are strongly dependent on core porosity, which has been shown to decrease with high thickness reductions and longer annealing times.

(3) The most detrimental influence on the critical current values are shear defects which are formed at high rolling reductions. This effectively places a limit on the extent to which porosity can be avoided by modifying the rolling processes.

(4) Loss of Tl through the metallic sheath is a possible mechanism for the observed increase in the volume fraction of secondary phase with longer annealing times, and this effect may explain the gradual decrease in critical current values at longer annealing times. The preferential formation of these Tl-free phases at the interface between the superconducting core and the AgNiMg sheath may be due to the presence of Ni and Mg reducing the nucleation energy of the secondary phases.

(5) The Tl-1223 grain structure can have a bimodal grain size distribution in *in situ* reacted tapes, and very large grains in melt processed tapes, but only by discovering a way to align these grains do we expect to increase the critical current values substantially.

The authors are grateful to Professor B. Cantor for the provision of laboratory facilities. P.D. was supported by the S.G.A. of the Slovak Academy of Sciences and for visits to the UK by the Royal Society under the Central and East European Collaborative Grants Scheme, and the Tl-tape programme is funded by the European Community under the Brite-Euram programme, contract number BRE2-CT93-0455.

References

- 1 T. Doi, M. Okada, A. Soeta, T. Yuasa, K. Aihara, T. Kamo and S. P. Matsuda, *Physica C*, 1991, **183**, 67.
- 2 D. N. Zheng, A. M. Campbell, R. S. Liu and S. P. Edwards, *Cryogenics*, 1993, **33**, 46.
- 3 M. R. Presland, J. L. Tallon, N. E. Plower, R. G. Buckley, A. Maudsley, M. P. Staines and M. G. Fee, *Cryogenics*, 1993, **33**, 502.
- 4 V. Selvamanickam, T. Finkle, K. Pfaffenbach, P. Haldar, E. J. Peterson, K. V. Salazaar, E. P. Roth and J. E. Tkaczyk, *Physica C*, 1996, **260**, 313.
- 5 Z. F. Ren and J. M. Wang, *Appl. Phys. Lett.*, 1992, **61**, 1715.
- 6 Z. F. Ren, C. A. Wang, J. H. Wang, D. J. Miller and K. C. Goretta, *Physica C*, 1994, **247**, 163.
- 7 Z. F. Ren and J. M. Wang, *Physica C*, 1993, **216**, 199.
- 8 D. N. Zheng, J. D. Johnson, A. R. Jones, A. M. Campbell, W. Y. Liang, T. Doi, M. Okada and K. Higashiyama, *J. Appl. Phys.*, 1995, **77**, 5287.
- 9 J. E. Everett, M. D. Johnston, G. K. Perkins, A. V. Volkozub, A. D. Caplin, J. C. Moore, S. Fox, D. Hyland and C. R. M. Grovenor, *IEEE Trans. Appl. Suppl.*, 1997.
- 10 R. E. Gladyshevsikii, A. Perin, B. Hensel, R. Flukiger, R. Abraham, K. Lebbou, M. Th. Cohen-Adad and J-L. Jordan, *Physica C*, 1995, **255**, 113.
- 11 S. Fox, J. C. Moore, R. Jenkins, C. R. M. Grovenor, V. Boffa, R. Bruzzese and H. Jones, *Physica C*, 1996, **257**, 332.
- 12 D. J. Miller, J. G. Hu, Z. Ren and J. H. Wang, *J. Electron. Mater.*, 1994, **23**, 1151.
- 13 J. C. Moore *et al.*, *Appl. Supercond.*, 1995, 483.
- 14 J. H. Richardson, in *Optical Microscopy for Materials Science*, Marcel Dekker, New York, 1971, p. 599.
- 15 J. C. Moore, D. Hyland, C. J. Salter, C. J. Eastell, S. Fox, C. R. M. Grovenor and M. J. Goringe, *Physica C*, in press.
- 16 A. Mogro-Campero, P. J. Bednarczyk, Y. Gao, R. B. Bolon, J. E. Tkaczyk and J. A. DeLuca, *Physica C*, 1996, **269**, 325.
- 17 M. R. Barron, in *Binary Phase Diagrams*, ed. T. B. Massalski, The Materials Information Society, 2nd edn., 1989, p. 108.
- 18 *CRC Handbook of Chemistry and Physics*, ed. R. C. Weast, CRC Press, Inc., Boca Raton, FL p. F-48.
- 19 S. Fox, J. C. Moore and C. R. M. Grovenor, *Inst. Phys. Conf. Ser.*, IOP, 1995, no. 148, p. 487.
- 20 Z. Cai and D. O. Welch, *Philos. Mag. B.*, 1994, **70**, 141.
- 21 F. J. Gottor, A. Fert, P. Odier and N. Pellerin, *Physica C*, 1994, **223-240**, 63.
- 22 P. Diko, I. Sargankova, M. Reissner and W. Steiner, *Physica C*, 1996, **269**, 22.

Paper 7/00850C; Received 5th February, 1997